Energy Current Cumulants in One-Dimensional Systems in Equilibrium

Abhishek Dhar,[1] Keiji Saito,[2] and Anjan Roy[3]
[1]International Centre for Theoretical Sciences, TIFR, Shivakote Village, Hesaraghatta Hobli, Bengaluru 560089, India
[2]Department of Physics, Keio University, Yokohama 223-8522, Japan
[3]The Abdus Salam International Center for Theoretical Physics, Strada Costiera 11, 34151 Trieste, Italy

(Received 9 December 2015; revised manuscript received 3 April 2018; published 31 May 2018)

A recent theory based on fluctuating hydrodynamics predicts that one-dimensional interacting systems with particle, momentum, and energy conservation exhibit anomalous transport that falls into two main universality classes. The classification is based on behavior of equilibrium dynamical correlations of the conserved quantities. One class is characterized by sound modes with Kardar-Parisi-Zhang scaling, while the second class has diffusive sound modes. The heat mode follows Lévy statistics, with different exponents for the two classes. Here we consider heat current fluctuations in two specific systems, which are expected to be in the above two universality classes, namely, a hard particle gas with Hamiltonian dynamics and a harmonic chain with momentum conserving stochastic dynamics. Numerical simulations show completely different system-size dependence of current cumulants in these two systems. We explain this numerical observation using a phenomenological model of Lévy walkers with inputs from fluctuating hydrodynamics. This consistently explains the system-size dependence of heat current fluctuations. For the latter system, we derive the cumulant-generating function from a more microscopic theory, which also gives the same system-size dependence of cumulants.

DOI: 10.1103/PhysRevLett.120.220603

The properties of energy and particle current fluctuations, in various systems both in and out of equilibrium, are areas of much recent activity. A number of papers have found unexpected universal features in these fluctuations in diverse systems [1–11]. For example, it has been shown that particle transfer in the symmetric exclusion process and charge transfer across disordered conductors have exactly the same value for a particular combination of current cumulants [9]. Systems with anomalous energy transfer have been of great interest both from the theoretical [12–14] and experimental [15,16] point of view and an open question is the properties of current fluctuations in such systems. An earlier study [11] considered a hard particle gas on a finite circle of length L and looked at the net energy q transferred across a point in a large time interval τ (taking the limit of fixed L and $\tau \to \infty$). Simulations indicated large fluctuations with the cumulants $\langle q^2 \rangle_c / \tau \sim L^{-1/2}$ and $\langle q^4 \rangle_c / \tau \sim L^{1/2}$, in sharp contrast to diffusive systems for which $\langle q^2 \rangle_c / \tau \sim L^{-1}$ and $\langle q^{2n} \rangle_c / \tau \sim L^{-2}$ for all $n > 1$.

In this Letter, we study energy current statistics in interacting particle systems with anomalous energy transport. We consider two different models, namely, the alternate mass hard particle gas [17–19] and the momentum exchange model [20,21]. In both cases, energy, momentum, and volume are conserved variables. These two models have been widely studied in the context of anomalous heat transport [13,14] where they represent examples of two universality classes. The thermal conductivity κ in such systems shows divergence with system size L as $\kappa \sim L^{\alpha}$, with $\alpha = 1/3$ or $1/2$ for the two classes. Recent work on the fluctuating hydrodynamic theory (FHT) [22–27] also predicts that these two models belong to different universality classes. One of the main aims of this Letter is to look at universal features of current fluctuations. We find from simulations that the two models give completely different results for fluctuations and show how the results can be understood from a simple model of Lévy walkers [28,29] with inputs from FHT, which allow us to compute the cumulant-generating function for current fluctuations (hence the large deviation function).

We consider N particles with positions and momenta described by $\{z_x, p_x\}$, for $x = 1, \ldots, N$, and moving on a periodic ring of size L, so that the particle density $\rho = N/L = 1$. The particles are assumed to only have nearest-neighbor interactions. In the alternate mass hard particle gas, point particles move ballistically in between energy-momentum conserving collisions. The masses of the particles are chosen as $m_{2x} = m_a$ and $m_{2x-1} = m_b$ for $x = 1, 2, \ldots, N/2$ (with N chosen to be even). The case $m_a = m_b$ is integrable, while for $m_a \neq m_b$ one numerically observes ergodicity and equilibration (for $N > 3$) [17–19], and it is expected that the system is nonintegrable. The system is taken to be in equilibrium (configurations are chosen from a microcanonical ensemble with fixed energy E and zero total momentum) at time $t = 0$, and we consider the statistics of the total energy transferred $q(y, \tau)$ across a specified point y in a given time interval τ. For the hard

particle gas, the energy flux at a spatial location y is given by $j(y,t) = \sum_{x=1}^{N} [m_x v_x(t)^3/2]\delta[y - z_x(t)]$.

The total energy flux in a fixed time interval is given by $q(y,\tau) = \int_0^\tau dt j(y,t)$, and our interest is in the statistics of this. On the ring geometry, the statistics is independent of y, and we can equivalently (for $\tau \gg L/c$, where c is the speed of sound) look at the statistics of the average integrated current, namely,

$$Q(\tau) = \frac{1}{L}\int_0^L dy q(y,\tau). \tag{1}$$

For the momentum exchange model [21], the Hamiltonian dynamics of a harmonic chain is supplemented by a stochastic process, which causes randomly chosen nearest-neighbor particles to exchange their momenta at a specified rate γ. Both energy (including now kinetic and potential energy parts) and momentum (and particle number) are conserved, and one can again define the energy current.

Simulations.—We evaluate up to six cumulants and compare them with the predictions of the theory. For the case of the hard-point gas, a system of $N = L$ particles was taken, with masses of alternate particles set at 1 and 2.62. This choice of mass ratio is not crucial, and anything not too close to 1 should work [30]. The initial velocities of the particles are chosen from a microcanonical ensemble, such that total momentum is zero and the total energy is $E = N$, which corresponds to a temperature $T = 2$ (with Boltzmann's constant $k_B = 1$). The initial positions of the particles are chosen from a uniform distribution between 0 and L. An event-driven molecular dynamics simulation was performed, in which successive update time steps are taken to be the time differences between subsequent collisions in the full chain. After some initial transients, the system is run for a total time of $R\tau$ and we obtain $Q_r(\tau)$ for $r = 1, 2, \ldots, R$. The nth moments are then computed as $C_n = \langle Q^n(\tau)\rangle = (1/R)\sum_{r=1}^{R} Q_r^n(\tau)$. We then compute the cumulants. The number of realizations averaged over was $R \sim \mathcal{O}(10^9)$.

Cumulants obtained from the two definitions of heat flux, Q in Eq. (1) or q, were evaluated. These behave differently at finite time, but both exhibit a linear growth for large τ and $\langle Q^n\rangle_c/\tau$ and $\langle q^n\rangle_c/\tau$ appear to converge to the same value, as is expected [11]. Here we show results only for Q. In Fig. (1), we show the time dependence of the cumulants for a system of size $N = 400$. Following [11], we plot the ratios $\langle Q_\tau^n\rangle_c/\tau$ versus $1/\tau$ and by extrapolating the linear region of the graph, extract the asymptotic values. These asymptotic values of the cumulants have been plotted in Fig. (2). We find

$$C_2 \sim N^{-1/2}, \quad C_4 \sim N^{1/2}, \text{ and } C_6 \sim N^{3/2}. \tag{2}$$

For $n = 2$ and 4, our results agree with those of [11], while those for $n = 6$ are new results.

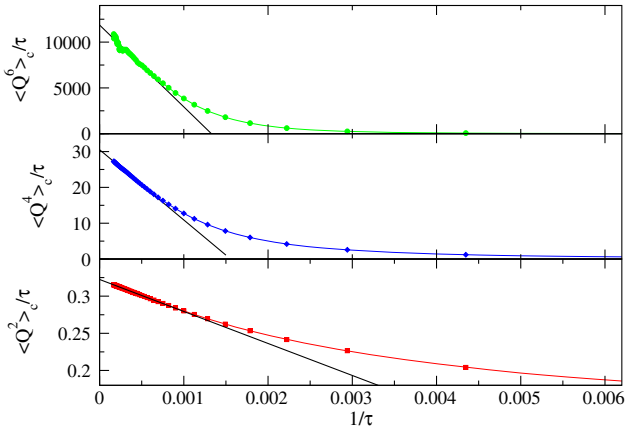

FIG. 1. Hard particle gas: plot of second, fourth, and sixth cumulants of integrated current divided by τ plotted against $1/\tau$ for a system of size $N = 400$. The solid lines indicate the extrapolation procedure used to obtain the asymptotic value of the cumulant.

For the momentum exchange model also, our simulations are done in the zero total momentum ensemble (with spring constants, masses set to one, and exchange rate $\gamma = 1$). In this case, it appears numerically challenging to study very large system sizes, possibly because the fluctuations are larger. Averages were done over $R \sim \mathcal{O}(10^7)$ realizations for sizes up to $N = 64$. However, in this model, asymptotic results are known to be reproduced even at relatively small system sizes [21]. The values of cumulants obtained by linear extrapolation have been plotted in Fig. (3). In this case, we find

$$C_2 \sim N^0, \qquad C_4 \sim N^2, \quad \text{and} \quad C_6 \sim N^4. \tag{3}$$

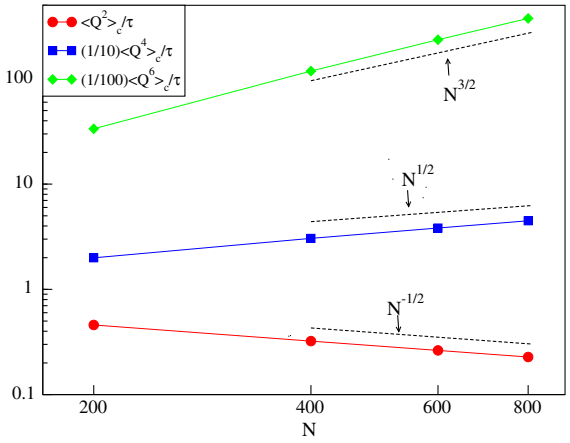

FIG. 2. Hard particle gas: plot of second, fourth, and sixth cumulants of the integrated energy current across a given point on a ring of size L with $N = L$ particles, in the alternate mass hard particle gas. The higher cumulants are multiplied by constant numbers to make the plots clearer. The dashed lines show the expected slopes.

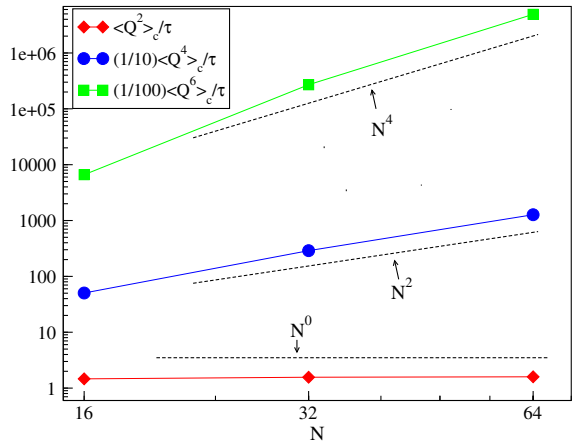

FIG. 3. Momentum exchange model: plot of second, fourth, and sixth cumulants of the integrated energy current across a given site on a ring with N particles. The higher cumulants are multiplied by constant numbers to make the plots clearer. The dashed lines show the expected slopes.

Note that for diffusive systems, one has $C_2 \sim N^{-1}$ and $C_{2n} \sim N^{-2}$ for all $n > 1$ [11]. Thus, systems with anomalous transport show a completely different scaling and fluctuations are much larger. Below, we will present arguments using the Lévy walk model [28,29], combining the results of FHT that, as we will see, explain the system-size dependencies completely. In addition, for the second model, we perform a more explicit microscopic calculation of the cumulant-generating function, which gives results consistent with the simulations and also the Lévy walk argument.

FHT and Lévy walk argument.—From the recent theory of FHT for 1D fluids, the picture emerges of the heat mode's diffusive spread being modified by interactions with sound modes, which themselves have Kardar-Parisi-Zhang scaling (and diffusive scaling for special conditions; see below). This interaction leads to the heat mode eventually showing Lévy scaling. One can thus think of the system as effectively a gas of independent Lévy walkers. Indeed, this approach has independently been used earlier to explain many observed features of anomalous transport [28,29]. To be precise, we assume the system to consist of a fixed number $N = \rho L$ of particles that perform independent Lévy walks on a ring of length L. At a microscopic level, the Lévy walker is a spontaneously formed heat packet, which then moves at speed c in either direction due to its coupling to the two sound modes. From FHT, a sound mode at wave vector k decays as $\sim \exp(-b|k|^\delta t)$ and this means that the heat packet will move in a given direction for a time interval t with probability $b|k|^\delta \exp(-b|k|^\delta t)$. Summing over all wave vectors, we then find that the distribution of flight times $\phi(t)$ of the Lévy walkers has a power-law tail: $\phi(t) \sim t^{-\beta+1}$ with $\beta = 1 + 1/\delta$. From FHT, the decay is given by $\delta = 3/2$ for the generic case, while $\delta = 2$ for the special case of zero pressure and even potentials (relevant for the harmonic exchange model). For a ring of finite size L, the smallest $k \sim L^{-1}$ and so the flight time distribution will have a cutoff at $\tau_L \sim L^\delta$. This is the timescale over which the sound mode spreads over the entire length of the system. With this basic picture, we now proceed to estimate the cumulants of the energy current.

As the walkers are independent, the cumulants of the integrated current Q are related to those of the displacement $x(\tau)$ of a single walker on the infinite line (in the steady state). The number of times that a single walker crosses a fixed point in the ring geometry is approximately $x(\tau)/L$. Hence, in the steady state, where the distribution of particles is uniform, the nth order of the cumulant is given by

$$\langle Q^n \rangle_c \sim \frac{N}{L^n} \langle x(\tau)^n \rangle_c = \frac{\rho}{L^{n-1}} \langle x(\tau)^n \rangle_c, \tag{4}$$

where ρ is the density on the ring. A straightforward computation of the truncated Lévy walk model then gives the following leading behavior for various moments: $\langle x^{2n} \rangle_c / (c^{2n}\tau) \sim \langle t^{2n} \rangle / \langle t \rangle$, $n = 1, 2, 3$, where $\langle t^{2n} \rangle = \int_0^{\tau_L} dt \phi(t) t^{2n}$ [31]. We now use these in Eq. (4) to obtain current fluctuations in the ring geometry. With the cutoff $\tau_L \sim L^\delta$, we get $\langle t^{2n} \rangle \sim L^{(2n-\beta)\delta}$, while $\langle t \rangle$ is a finite number; hence, we get

$$\frac{\langle Q^{2n} \rangle_c}{\tau} \sim L^{(2n-\beta)\delta-(2n-1)} \quad n = 1, 2, 3. \tag{5}$$

In general, we conjecture this result to be true for all n. We then immediately find that the choices $(\beta, \delta) = (5/3, 3/2)$ and $(3/2, 2)$ reproduce the observed results for cumulants in the hard-particle gas and the exchange model, respectively.

More explicit analysis for the momentum exchange model.—In the framework of FHT, the second model we studied corresponds to the special case of a symmetric potential and zero pressure and belongs to a different universality from the generic cases [24]. In this case, the sound modes obey the diffusion equation, while the heat mode is affected by nonlinear coupling to the sound modes. Assuming Gaussian fluctuations of the sound modes, we expect the stretch and momentum variables $r(x, t)$ and $p(x, t)$ to satisfy the following Langevin equations,

$$\begin{aligned} \frac{\partial r(x,t)}{\partial t} &= \nabla[p(x,t)], \\ \frac{\partial p(x,t)}{\partial t} &= \nabla[c^2 r(x-1,t) + D\nabla[p(x-1,t)] + B\eta(x,t)], \end{aligned} \tag{6}$$

where the symbol ∇ is the discrete derivative that acts as $\nabla[A(x)] := A(x+1) - A(x)$ for arbitrary function A. The variable $\eta(x, t)$ is white Gaussian noise with unit variance

and the strength $B = \sqrt{2D}$ ensures that equal-time correlations at long times converge to the expected equilibrium values, e.g., $c^2\langle r(x,t)r(0,t)\rangle = \langle p(x,t)p(0,t)\rangle = \delta_{x,0}$. In fact, the two time correlations from these equations also agree with the known exact form. Note that Eqs. (6) are not microscopic equations, but hydrodynamic equations. There is a third equation for the other hydrodynamic field, namely, the energy, with a corresponding conserved current (see [24]). The dominant part of the energy current is given by $j_e(x,t) = -c^2 r(x,t)p(x,t)$. This scales as $1/\sqrt{N}$, while the stochastic component scales as $1/N$. With the assumption that the fields r, p are described by (6), we now proceed to evaluate the distribution of the current. We define the discrete Fourier transform $\tilde{r}(q,\omega) = \sum_{x=1}^{N}\int_0^\tau dt r(x,t)e^{-i(qx-\omega t)}/(N\tau)$, where $q = 2s\pi/N$ and $\omega = 2n\pi/\tau$ and similar for the momentum and noise terms. Plugging the Fourier representation of each variable into (6), we solve for the stretch and momentum variables in terms of noise variables,

$$\tilde{p}(q,\omega) = \frac{-i\omega B_p(e^{-iq}-1)\tilde{\eta}(q,\omega)}{-\omega^2 + 2c^2\lambda_q + 2i\omega D_p\lambda_q}, \tag{7}$$

$$\tilde{r}(q,\omega) = \frac{i(e^{-iq}-1)\tilde{p}(q,\omega)}{\omega}, \tag{8}$$

where $\lambda_q = 2(1-\cos q)$ and the noise correlations are given by $\langle\tilde{\eta}(q,\omega)\tilde{\eta}(q',\omega')\rangle = \delta_{q+q'}\delta_{\omega+\omega'}/(N\tau)$.

The average integrated current Q can then be written as

$$\begin{aligned} Q &= \frac{c^2}{N}\sum_{l=1}^{N}\int_0^\tau dt r(x,t)p(x,t) \\ &= c^2\tau\sum_{q,\omega}\tilde{r}(q,\omega)\tilde{p}(-q,-\omega) \\ &= \tau\sum_{q\neq 0}\sum_{\omega}A(q,\omega)\tilde{\eta}(q,\omega)\tilde{\eta}(-q,-\omega), \end{aligned} \tag{9}$$

where $A(q,\omega)$ is given by

$$A(q,\omega) = -\frac{4D_p c^2\omega\sin q\lambda_q}{(\omega^2-2c^2\lambda_q)^2 + 4D_p^2\omega^2\lambda_q^2}. \tag{10}$$

The characteristic function $Z(\lambda) := \langle e^{-\lambda Q}\rangle$, where the average is over the Gaussian noise $\tilde{\eta}(q,\omega)$, leads to

$$\begin{aligned} Z(\lambda) &= \prod_q\prod_\omega\langle e^{-\lambda\tau A(q,\omega)\tilde{\eta}(q,\omega)\tilde{\eta}(-q,-\omega)}\rangle \\ &= \prod_q\prod_\omega\frac{N\tau}{N\tau+\lambda\tau A(q,\omega)}. \end{aligned} \tag{11}$$

For large τ, the function $Z(\lambda)$ has the large deviation form $Z(\lambda)\sim e^{\mu(\lambda)\tau}$, with the cumulant-generating function given by

$$\begin{aligned} \mu(\lambda) = -\frac{1}{2\pi}\sum_{q\neq 0}\int_{-\infty}^{\infty}d\omega \\ \times\log\left(1-\frac{\lambda}{N}\frac{4D_p c^2\omega\sin q\lambda_q}{(\omega^2-2c^2\lambda_q)^2+4D_p^2\omega^2\lambda_q^2}\right). \end{aligned} \tag{12}$$

It is difficult to perform this integration explicitly, but the system-size dependence of the cumulants, given by $(\langle Q^n\rangle_c/\tau) = \partial^n\mu(\lambda)/\partial\lambda^n|_{\lambda\to 0}$, can be evaluated to give

$$\frac{\langle Q_{2n}\rangle_c}{\tau} = \frac{1}{N^{2n}}\sum_{q\neq 0}\frac{\left[4D_p c^2\sin q\lambda_q\right]^{2n}(2n-1)!}{2\pi}I_{2n}, \tag{13}$$

$$I_{2n} = \int_{-\infty}^{\infty}d\omega\frac{\omega^{2n}}{\left[(\omega^2-2c^2\lambda_q)^2+4D_p^2\omega^2\lambda_q^2\right]^{2n}}. \tag{14}$$

In particular, we find

$$I_2 = \frac{\pi}{2ab^3}, \qquad I_4 = \frac{(b^2+5a)\pi}{16a^3b^7},$$
$$I_6 = \frac{(3b^4+21ab^2+63a^2)\pi}{256a^5b^{11}},$$

where $a = 2c^2\lambda_q$ and $b = 2D_p\lambda_q$ [32]. Taking the continuum limit, we set $\lambda_q = q^2$ with $q = 2s\pi/N$. Then we get $\langle Q_2\rangle_c/\tau\sim N^0$, $\langle Q_4\rangle_c/\tau\sim N^2$, and $\langle Q_4\rangle_c/\tau\sim N^4$, which reproduces the results from simulations and also the Lévy walk argument.

Summary.—Recently, using FHT, it has been shown that generic one-dimensional systems with conserved density, momentum, and energy show anomalous transport and can be classified into two principal universality classes. So far, the signatures of anomalous transport and different universality classes have been seen in studies on decay of equilibrium correlations and in nonequilibrium transport measurements where one looks at scaling of current with system size. In the present Letter, we show that current fluctuations in equilibrium provide another method for identifying anomalous transport behavior and identifying universality classes. We presented results of numerical simulations showing that the system-size scaling of energy current cumulants is completely different for the two universality classes predicted by FHT and also differs from that for diffusive systems. This is explained by a phenomenological model where the energy is carried by Lévy walkers with lifetimes determined by interactions with sound modes. For the momentum exchange model, which is in the same universality class as systems with an even potential and zero pressure, we recover the scaling properties from a direct microscopic computation of the cumulant-generating function.

It is of interest to see if results on current statistics in other systems described by FHT [33,34] can also be obtained using the ideas proposed here.

We are grateful to Bernard Derrida and Henk van Beijeren for their many valuable suggestions and critical comments on the manuscript. A. D. acknowledges support from UGC-ISF Indo-Israeli research Grant No. 6-8/2014 (IC) and the Grant EDNHS ANR-14-CE25-0011 of the French Ministry of Education. K. S. was supported by JSPS (No. 26400404). We thank the Galileo Galilei Institute for Theoretical Physics for the hospitality and the INFN for partial support during the initiation of this work. We thank the NESP program (ICTS/Prog-NESP/2015/10) at the International Centre for Theoretical Sciences, TIFR, where this work was largely completed.

[1] T. Bodineau and B. Derrida, Phys. Rev. Lett. **92**, 180601 (2004).
[2] E. Akkermans, T. Bodineau, B. Derrida, and O. Shpielberg, Europhys. Lett. **103**, 20001 (2013).
[3] B. Derrida, B. Doucot, and P.-E. Roche, J. Stat. Phys. **115**, 717 (2004).
[4] H. Lee, L. S. Levitov, and A. Y. Yakovets, Phys. Rev. B **51**, 4079 (1995).
[5] K. Saito and A. Dhar, Phys. Rev. Lett. **99**, 180601 (2007).
[6] B. Derrida and J. L. Lebowitz, Phys. Rev. Lett. **80**, 209 (1998).
[7] B. Derrida and C. Appert, J. Stat. Phys. **94**, 1 (1999).
[8] C. Appert-Rolland, B. Derrida, V. Lecomte, and F. van Wijland, Phys. Rev. E **78**, 021122 (2008).
[9] P. E. Roche, B. Derrida, and B. Doucot, Eur. Phys. J. B **43**, 529 (2005).
[10] L. Bertini, A. De Sole, D. Gabrielli, G. Jona-Lasinio, and C. Landim, Rev. Mod. Phys. **87**, 593 (2015).
[11] E. Brunet, B. Derrida, and A. Gerschenfeld, Europhys. Lett. **90**, 20004 (2010).
[12] S. Lepri, *Thermal Transport in Low Dimensions: From Statistical Physics to Nanoscale Heat Transfer*, Lecture Notes in Physics Vol. 921 (Springer, Heidelberg, 2016).
[13] S. Lepri, R. Livi, and A. Politi, Phys. Rep. **377**, 1 (2003).
[14] A. Dhar, Adv. Phys. **57**, 457 (2008).
[15] C. W. Chang, D. Okawa, H. Garcia, A. Majumdar, and A. Zettl, Phys. Rev. Lett. **101**, 075903 (2008).
[16] V. Lee, C. H. Wu, Z. X. Lou, W. L. Lee, and C. W. Chang, Phys. Rev. Lett. **118**, 135901 (2017).
[17] P. L. Garrido, P. I. Hurtado, and B. Nadrowski, Phys. Rev. Lett. **86**, 5486 (2001).
[18] A. Dhar, Phys. Rev. Lett. **88**, 249401 (2002).
[19] P. Grassberger, W. Nadler, and L. Yang, Phys. Rev. Lett. **89**, 180601 (2002).
[20] G. Basile, C. Bernardin, and S. Olla, Phys. Rev. Lett. **96**, 204303 (2006).
[21] S. Lepri, C. Mejía-Monasterio, and A. Politi, J. Phys. A **42**, 025001 (2009).
[22] H. van Beijeren, Phys. Rev. Lett. **108**, 180601 (2012).
[23] C. B. Mendl and H. Spohn, Phys. Rev. Lett. **111**, 230601 (2013).
[24] H. Spohn, J. Stat. Phys. **154**, 1191 (2014).
[25] C. B. Mendl and H. Spohn, Phys. Rev. E **90**, 012147 (2014).
[26] S. G. Das, A. Dhar, K. Saito, C. B. Mendl, and H. Spohn, Phys. Rev. E **90**, 012124 (2014).
[27] V. Popkov, A. Schadschneider, J. Schmidt, and G. M. Schütz, Proc. Natl. Acad. Sci. U.S.A. **112**, 12645 (2015).
[28] S. Lepri and A. Politi, Phys. Rev. E **83**, 030107 (2011).
[29] A. Dhar, K. Saito, and B. Derrida, Phys. Rev. E **87**, 010103 (R) (2013).
[30] S. Chen, J. Wang, G. Casati, and G. Benenti, Phys. Rev. E **90**, 032134 (2014).
[31] A. Dhar and K. Saito, Phys. Rev. E **87**, 010103 (2013).
[32] For general n, we find $I_{2n} \sim (1/\lambda_q)^{5n-1}$.
[33] M. Kulkarni, D. A. Huse, and H. Spohn, Phys. Rev. A **92**, 043612 (2015).
[34] V. Popkov, J. Schmidt, and G. M. Schütz, Phys. Rev. Lett. **112**, 200602 (2014).